U.R.S.I. FRANCE JS 20 FUTURE NETWORKS: 5G AND BEYOND

Conversion of a Pulsed Source Using a Multiband Frequency Selective Surface for HPM Applications

Modification d'une Source Impulsionnelle via Surface Sélective en Fréquence Multibande pour des Applications HPM

Fernando Albarracin-Vargas[1], Felix Vega[1,2], Chaouki Kasmi[1,3], David Martinez[1], Fahad Alyafei[1], Lars-Ole Fichte[2]

[1] *Directed Energy Research Centre, TII, Abu Dhabi, United Arab Emirates, fernando.albarracin@tii.ae*
[2] *Universidad Nacional de Colombia - Sede Bogotá, Bogotá, Colombia, jfvegas@unal.edu.co*
[3] *Faculty of Electrical Engineering, Helmut Schmidt University, Hamburg, Germany, lo.fichte@hsu-hh.de*

Keywords (in English and French): frequency selective surface, impulse radiating antenna, complementary split-ring resonator/surface sélective en fréquence, antenne à rayonnement impulsionnel, résonateur à anneau fendu complémentaire.

Abstract/Résumé

This paper presents a new contribution to a recently introduced type of resonant radiator, obtained as a combination of a Frequency Selective Surface (FSS) and an Impulse Radiating Antenna. The effects of a multiband FSS is studied and verified via simulations. A multiband radiator is obtained, enabling the capability of modifying the emitted signal for multiple applications, like EMI testing, or development of hardening modules that could be integrated into facilities. / Cet article présente une nouvelle méthode permettant la création d´une source micro-onde obtenu en combinant une surface sélective en fréquence (FSS) et une antenne à rayonnement impulsionnel. Les effets d'une FSS multibande sont étudiés et vérifiés via des simulations. Cette combinaison permet de modifier le signal émis par une source impulsionnelle résultant en une source micro-onde de forte puissance.

1 Introduction

The radiation of high-power electromagnetic pulses (EMP), produced by High Power Microwave (HPM) sources, is a topic of significant interest for the academic community and defense industry. It is related to the potential disruption of electrical systems and high technology microcircuits, both part of the critical infrastructure of a country. The characterization of such disruptions is subject to the Intentional Electromagnetic Interference (IEMI) studies. A key part of the design of a high-power EMP radiator is the antenna system [1], which involves the use of radiators with both broad bandwidth and high-voltage handling capabilities. The Impulse Radiating Antenna (IRA), first proposed by Baum and Farr [2]–[4], is one of the most representative types of high-power pulsed radiators for IEMI tests, due to its hyper-band response and high-power capability.

Both components mentioned so far, the antenna and the HPM pulsed source, share two important characteristics: high cost and fixed working bandwidth. In this context, the use of a frequency selective planar structure arises as a strategy to add frequency agility to the complete system ntenna+EMP source. The ability to radiate over multiple bands is possible by arranging multiple resonating unit-cell types/dimensions into the Frequency Selective Surfaces (FSS). A thorough study regarding the band-stop effect from the metal-based grid of building walls, when illuminated with a hyper-band radiator, has been reported in [5]. The attenuation effect, due to reinforced concrete walls, in the downlink bands of actual mobile communication systems, is studied in [6]. A low-pass FSS that can be integrated into an ultra-wideband radiator was presented in [7]. Other alternatives, like the use of self-actuated surfaces, using arrays of nonlinear devices are described in [8], [9]. Voltage-controlled piezoelectric actuators are used to tune an FSS in [10].

FSS are narrowband passive structures that expose interesting properties when illuminated by electromagnetic fields. In their more usual form, the FSSs are implemented as resonant metal elements, or apertures, electrically small as compared with its resonance frequency, placed periodically over a containing surface or substrate [11]. The well-known Split Ring Resonators (SRR) proposed in [12] and its complementary version (i.e., CSRR), have been studied and characterized in the last years as a compact structure to compose an FSS [11], [13]. Frequency Selective Surfaces (FSS) are narrowband passive structures. In their more usual form, the FSSs are

implemented as resonant metal elements, or apertures, electrically small with respect to its resonance frequency, placed periodically over a containing surface or substrate [11]. To avoid diffractive effects and grating-lobes on the intended radiated beam, both the unit cell size and the periodicity separation shall be smaller than the wavelength of the incident radiation.

The well-known Split Ring Resonators (SRR) proposed in [12] and its complementary version (i.e. CSRR), have been studied and characterized in the last years as a compact structure to compose an FSS [13]. A very relevant characteristic of this resonators, for the sake of this work, is the capability of being cross-polarized. Thus, for the case of the SRR, a polarizing surface results by either the E- or the H- field (or both) polarized in a certain direction [11], a band-stop response of the FSS is obtained. Similarly, an electric dipole is induced from the excitation of a CSRR with an incident wave with the E-field component parallel to the rings' gaps, resulting in a bandpass filter surface. Marques et al. [11] presented an analytical solution for the behavior of the SRR- and CSRR-based FSS. Although restricted to the infinitesimally thin perfect conductor in free space, the analytical approach gives a first approximation to the response of a band-pass-type FSS.

This work presents an integrated multiband radiator by locating a CSRR-FSS in the near-field of an IRA as a strategy to add waveform and frequency agility to the EMP source. The ability to radiate over multiple bands is possible by arranging multiple-size resonating unit-cell into the FSS.

2 Multiband FSS Design

2.1 Unit Cell Design

The proposed unit cell is to be supported by a low relative permittivity substrate, (ideally $\varepsilon_r = 1$), simulated as losses free as a first approximation. It is composed of two different CSRRs, oriented as shown in Figure 1b. Since the intended response of the FSS is multiband, each band shall be tuned according to the resonant frequency of each unit-cell size. Only waves whose E-field is aligned to the gaps in the rings (*y*-axis in Figure 1a) will be able to pass through the FSS, at frequencies slightly higher than the resonant frequencies of the composing CSRR sizes. Figure 2 shows the reflection and the transmission parameter, respectively, for the unconnected CSRR-based FSS presented in this work. An additional resonant frequency is observed at 2.6 GHz in Figure 2b. This is associated with a high-frequency resonance of the 1.5 GHz unit cell. This additional passband is expected to be overlapped with the response from the 2.4 GHz unit cell.

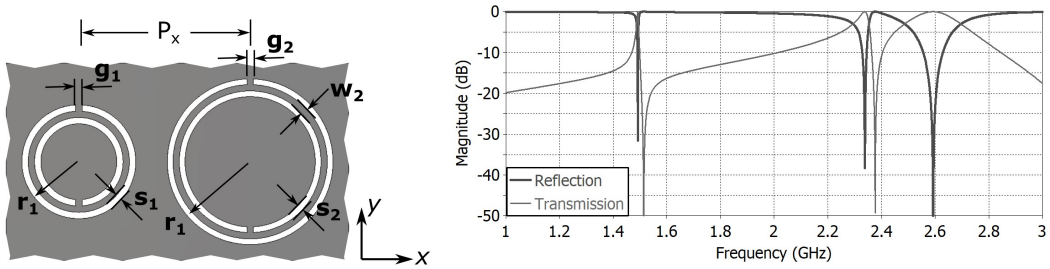

(a) (b)

Figure 1: (a) Sketch of the two CSRR unit cells geometry. Unit cell 1, on the left, is associated with a passband frequency of 2.4 GHz. The unit cell on the right is resonant at 1.5 GHz. The dimensions are (all in mm) P_x= 26.5, P_y= 26.5, r_1 = 8.5, r_2 = 12.65, g_1 = g_2 = 1, s_1= s_2= 1, w_1= w_2= 1. (b) FSS response, simulated as an infinite periodic structure

2.2 Reflector Based IRA

The sketch of a two-arm IRA is shown in Figure 2a. When connected to a pulsed voltage source, the IRA radiates an impulse-like waveform over a narrow beam in the boresight direction (*z*-axis in Figure 2a). The electric field related to the waveform radiated by the IRA can be described as:

$$E_t(t,r) = f_1 \frac{1}{2\pi f_g} \begin{pmatrix} \frac{V(t-r/c)}{r}\frac{\sin(\beta)}{1+\cos(\beta)} - \frac{V(t-l/c-R_2/c)}{R_2}\frac{\sin(\beta)+\sin(\gamma)}{1+\cos(\beta-\gamma)} \\ -\frac{4}{D}V(t-2F/c-r/c)+(2+2\cos(\gamma))\frac{V(t-l/c-R_2/c)}{D} \end{pmatrix} (V/m) \quad (1)$$

where: V(t) is the feeding voltage, c is the speed of light and r is the distance between the focal point and the measurement point. The geometric impedance factor, $f_g = Z_{IRA}/120\pi$, is a reference parameter related to the feeder geometry that transmits the quasi-spherical TEM wave into the reflector. Z_{IRA} is the input impedance of the antenna. *D, F, l*, β, γ, and R_2, are described in Figure 2a. The two-arm coplanar feeder IRA presented in this paper is designed with the following parameters: D= 1(m), F/D =0.4, Z_{IRA}= 400 (Ω).

2.3 Radiator Integration

The multiband radiator proposed here is depicted in Figure 2b. The FSS acts as a passband filter with a high-Q factor response. As mentioned before, the FSS is acting as a bandpass filter, modifying the impulse-like waveform propagating from the IRA by converting it into a dumped sinusoidal, with two different frequency components. Only the E-field components aligned with the y-axis, and around the resonant frequency of each unit cell, will effectively pass through the FSS. Unit cells of the same size are aligned along the y-axis, in order to align each resonant polarization with the incoming wideband transient wave from the IRA.

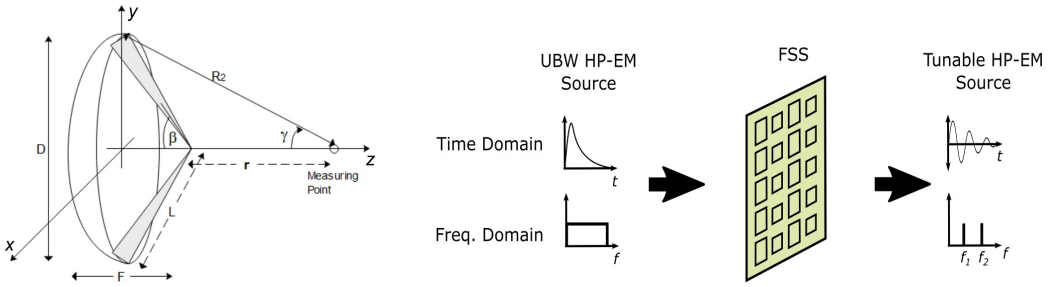

(a) (b)

Figure 2: (a) Reflector-based IRA geometry. (b) Multiband HMP Radiator scenario

3 Results

The proposed integrated multiband radiator is modeled in a commercial full-wave simulator. The FSS is located 10 cm away from the focal point of the IRA. Although a large separation between FSS and antenna would minimize multiple reflections, diffracted waves from the perimeter of the FSS structure will have a more significant effect in the filtered pulse.

The E-field has been computed 5 m away from the focal point of the IRA, in broadside (*z*-axis). The time-domain response of the radiated E-field is shown in Figure 3a. The field radiated by a conventional two-arm unloaded IRA, with the same dimensions, is also shown as a reference. In both cases, a Gaussian pulse, with spectral content ranging from 0 to 3.5 GHz and unity amplitude is used as the driving signal.

It is observed the damped-like sinusoidal response of the proposed design, as expected. The passband filter behavior of the FSS loading the IRA is seen in the frequency domain response of the electric field, as shown in Figure 3b. The ideal filtering response of the IRA+FSS system can be computed as a cascaded product of the transfer functions, in the frequency domain, of the IRA and the FSS. This is possible by applying the *chain parameters* approach [6], as

$$T_A(f) = E_{IRA}(f)/V_{in}(f) \quad (2)$$

$$\begin{aligned} T_{Total}(f) &= T_A(f)T_{FSS}(f) \\ E_{IRA+FSS}(f) &= T_{Total}(f)V_{in}(f) \end{aligned} \quad (3)$$

where $V_{in}(f)$ and $E_{IRA}(f)$ are the Fourier transform of the voltage driving the IRA, and the radiated field, respectively. $T_{FSS}(f)$ can be computed from the *S*-parameters of the FSS. Note that the $E_{IRA}(f)$ does not necessarily have to be computed in the far-field region.

Despite the amplitude drop in the full-wave simulated IRA+FSS response, the intended passband effect holds around the resonant frequency of each unit-cell size, as can be seen in Figure 3b. Ideally, the impulse-like radiated pulse shall be converted into a signal with two different frequency components. However, harmonic resonances from the unit cells limit the bandwidth operation of the integrated radiator.

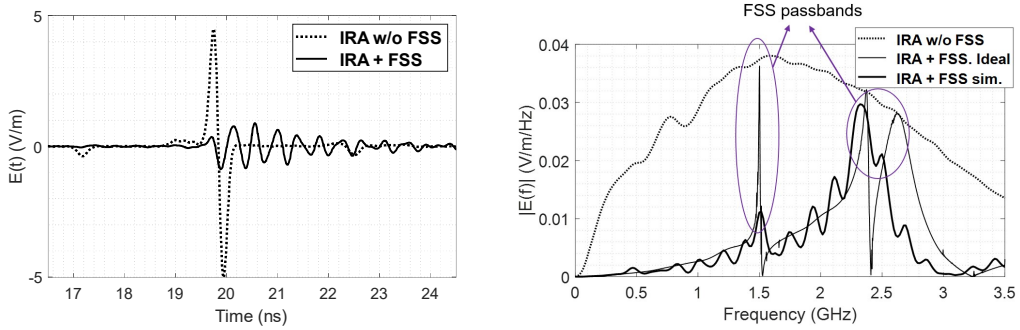

(a) (b)

Figure 3: IRA vs. IRA+FSS: (a) time-domain and (b) spectral magnitude response in farfield, on boresight.

Since the proposed multiband FSS presents bilateral symmetry with respect to the main planes around the axis of the IRA, i.e., *xz*-plane and *yz*-plane in Figure 2a, a symmetric and still directive radiation pattern can be expected, as it is shown in Figure 4. Significant degradation in the SLL ratio is observed in both frequency bands, especially in the *E*-plane. This can be associated with the limited size of the FSS (1 x 1 m^2) that was finally integrated into the radiator. Thus, the effects of diffraction due to the FSS edge are evident. At higher frequencies (i.e. 2.4 GHz) this phenomenon is less arresting but still significant. One possible solution for this problem can be simply increasing the total area of the FSS, at the expense of affecting the manageability of the radiator. The maximum directivity is decreased from 18 dBi to 11 dBi at 1.5 GHz, while remained 22 dBi at 2.4 GHz. This response is in accordance with the higher field strength around 2.4 GHz, once the wave passes through the FSS (see Figure 3b).

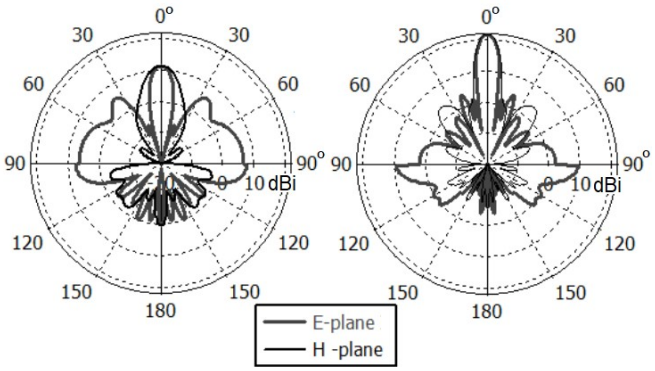

Figure 4: Radiation response of the integrated radiator, IRA+FSS. (a) At 1.5 GHz, (b) at 2.4 GHz.

An integrated multiband radiator has been presented. Multiband high-power radiation is enabled by adding frequency-selective planar structures to hyper-band radiators, like the two-arm IRA. Computed results in terms of the field strength, spectral density of the electric field, and the radiation pattern of the integrated antenna system have been obtained. The implementation of a prototype to verify the design is under process.

References

[1] F. Vega, N. Mora, F. Rachidi, N. Pena, and F. Roman, "Design, Construction and Test of a Half Impulse Radiating Antenna (HIRA)Canada.," in *American Electromagnetics Conference [AMEREM]*, Otawa, 2010.

[2] C. E. Baum, "Radiation of Impulse-Like Transient Fields," *Sens. Simul. Notes*, vol. 321, no. USAF Philiips Lab, p. 28, Nov. 1989.

[3] C. E. Baum and E. G. Farr, "Impulse Radiating Antennas," in *Ultra-Wideband, Short-Pulse Electromagnetics 2*, H. L. Bertoni, L. Carin, and L. B. Felsen, Eds. Boston, MA: Springer US, 1993, pp. 139–147.

[4] C. E. Baum, "Aperture Efficiencies for IRAs," *Sens. Simul. Notes*, no. 328, Jun. 1991.

[5] F. M. Tesche and D. V. Giri, "Modification of Impulse-Radiating Antenna Waveforms for Infrastructure Element Testing," *Sens. Simul. Notes*, vol. 572, p. 25.

[6] G. Antonini, A. Orlandi, and S. D'elia, "Shielding effects of reinforced concrete structures to electromagnetic fields due to GSM and UMTS systems," *IEEE Trans. Magn.*, vol. 39, no. 3, pp. 1582–1585, May 2003, doi: 10.1109/TMAG.2003.810327.

[7] W. Bigelow, E. G. Farr, and J. S. Tyo, "A Frequency Selective Surface Used as a Broadband Filter to Pass Low-Frequency UWB while Reflecting X–Band Radar," *Sens. Simul. Notes*, no. 506, 2006.

[8] C. Yang, P.-G. Liu, and X.-J. Huang, "A Novel Method of Energy Selective Surface for Adaptive HPM/EMP Protection," *IEEE Antennas Wirel. Propag. Lett.*, vol. 12, pp. 112–115, 2013, doi: 10.1109/LAWP.2013.2243105.

[9] S. Monni *et al.*, "Limiting frequency selective surfaces," in *2009 European Microwave Conference (EuMC)*, 2009, pp. 606–609, doi: 10.23919/EUMC.2009.5296360.

[10] M. Mavridou, K. Konstantinidis, A. Feresidis, and P. Gardner, "Novel tunable frequency selective meta-surfaces," in *2016 46th European Microwave Conference (EuMC)*, 2016, pp. 301–304, doi: 10.1109/EuMC.2016.7824338.

[11] R. Marques *et al.*, "Ab initio analysis of frequency selective surfaces based on conventional and complementary split ring resonators," 2005, doi: 10.1088/1464-4258/7/2/005.

[12] J. B. Pendry, A. J. Holden, D. J. Robbins, and W. J. Stewart, "Magnetism from conductors and enhanced nonlinear phenomena," *IEEE Trans. Microw. Theory Tech.*, vol. 47, no. 11, pp. 2075–2084, Nov. 1999, doi: 10.1109/22.798002.

[13] J. D. Ortiz, J. D. Baena, V. Losada, F. Medina, and J. L. Araque, "Spatial Angular Filtering by FSSs Made of Chains of Interconnected SRRs and CSRRs," *IEEE Microw. Wirel. Compon. Lett.*, vol. 23, no. 9, pp. 477–479, Sep. 2013, doi: 10.1109/LMWC.2013.2274997.